


# Effect of macrophage-to-myofibroblast transition on silicosis

Fei Geng<sup>1,2</sup> | Jingrou Xu<sup>1</sup> | Xichen Ren<sup>1</sup> | Ying Zhao<sup>1</sup> | Yuhao Cai<sup>1</sup> | Yaqian Li<sup>1</sup> | Fuyu Jin<sup>1</sup> | Tian Li<sup>1</sup> | Xuemin Gao<sup>1</sup> | Wenchen Cai<sup>1</sup> | Hong Xu<sup>1</sup>  | Zhongqiu Wei<sup>2</sup>  | Na Mao<sup>1</sup> | Ying Sun<sup>2</sup> | Fang Yang<sup>1</sup>

<sup>1</sup>Hebei Key Laboratory for Organ Fibrosis Research, School of Public Health, North China University of Science and Technology, Tangshan, China

<sup>2</sup>Department of Pathology, Hebei Key Laboratory for Chronic Diseases, School of Basic Medical Sciences, North China University of Science and Technology, Tangshan, China

## Correspondence

Na Mao and Fang Yang, Hebei Key Laboratory for Organ Fibrosis Research, School of Public Health, North China University of Science and Technology, Tangshan, China.  
Email: maona@ncst.edu.cn and fangyang@ncst.edu.cn

Ying Sun, Department of Pathology, Hebei Key Laboratory for Chronic Diseases, School of Basic Medical Sciences, North China University of Science and Technology, Tangshan, China.  
Email: sunying@ncst.edu.cn

## Funding information

Provincial Graduate Student Innovation Funding Project of Hebei Province, Grant/Award Number: CXZZBS2022104; Science and Technology of Project of Hebei Education Department, Grant/Award Number: QN2022009; National Natural Science Foundation of China, Grant/Award Number: 82204006; National Natural Science Foundation of Hebei Province, Grant/Award Number: H2020209292 and H2024209038

## Abstract

**Background:** The aim was to explore the effect of macrophage polarization and macrophage-to-myofibroblast transition (MMT) in silicosis.

**Methods:** Male Wistar rats were divided into a control group and a silicosis group developed using a HOPE MED 8050 dynamic automatic dusting system. Murine macrophage MH-S cells were randomly divided into a control group and an SiO<sub>2</sub> group. The pathological changes in lung tissue were observed using hematoxylin and eosin (HE) and Van Gieson (VG) staining. The distribution and location of macrophage marker (F4/80), M1 macrophage marker (iNOS), M2 macrophage marker (CD206), and myofibroblast marker ( $\alpha$ -smooth muscle actin [ $\alpha$ -SMA]) were detected using immunohistochemical and immunofluorescent staining. The expression changes in iNOS, Arg,  $\alpha$ -SMA, vimentin, and type I collagen (Col I) were measured using Western blot.

**Results:** The results of HE and VG staining showed obvious silicon nodule formation and the distribution of thick collagen fibers in the lung tissue of the silicosis group. Macrophage marker F4/80 increased gradually from 8 to 32 weeks after exposure to silica. Immunohistochemical and immunofluorescent staining results revealed that there were more iNOS-positive cells and some CD206-positive cells in the lung tissue of the silicosis group at 8 weeks. More CD206-positive cells were found in the silicon nodules of the lung tissues in the silicosis group at 32 weeks. Western blot analysis showed that the expressions of Inducible nitric oxide synthase and Arg protein in the lung tissues of the silicosis group were upregulated compared with those of the control group. The results of immunofluorescence staining showed the co-expression of F4/80,  $\alpha$ -SMA, and Col I, and CD206 and  $\alpha$ -SMA were co-expressed in the lung tissue of the silicosis group. The extracted rat alveolar lavage fluid revealed F4/80<sup>+</sup> $\alpha$ -SMA<sup>+</sup>, CD206<sup>+</sup> $\alpha$ -SMA<sup>+</sup>, and F4/80<sup>+</sup> $\alpha$ -SMA<sup>+</sup>Col I<sup>+</sup> cells using immunofluorescence staining. Similar results were also found in MH-S cells induced by SiO<sub>2</sub>.

**Conclusions:** The development of silicosis is accompanied by macrophage polarization and MMT.

Fei Geng, Jingrou Xu, and Xichen Ren are co-first authors.

This is an open access article under the terms of the Creative Commons Attribution-NonCommercial-NoDerivs License, which permits use and distribution in any medium, provided the original work is properly cited, the use is non-commercial and no modifications or adaptations are made.

© 2024 The Author(s). *Animal Models and Experimental Medicine* published by John Wiley & Sons Australia, Ltd on behalf of The Chinese Association for Laboratory Animal Sciences.

## KEYWORDS

macrophage, macrophage-to-myfibroblast transition, silicosis

## 1 | INTRODUCTION

Silicosis is a public health challenge as it is the most common occupational disease globally, but no curative treatment has yet been proposed in clinical practice.<sup>1-3</sup> It is widely acknowledged that pulmonary macrophages have an effect in regulating the fibrotic response, as they are involved in clearing pathogens and maintaining steady-state homeostasis.<sup>4,5</sup> Macrophages in lung tissue include both classically activated macrophages (M1) and alternatively activated macrophages (M2). Recent studies have revealed novel findings that bone marrow-derived monocytes/macrophages have the capacity to transform into collagen-producing myofibroblasts.<sup>6-9</sup> The characteristic of the transformation is the co-expression of macrophage markers (F4/80 or CD68) and myofibroblast marker  $\alpha$ -smooth muscle actin ( $\alpha$ -SMA). These findings were first observed in unilateral ureteral obstruction.<sup>10,11</sup> These studies suggest that macrophage-to-myfibroblast transition (MMT) could be an alternative pathway for the regulation of fibrosis. Nonetheless, the influence of macrophage polarization and MMT in silicosis remains elusive.

The present study employed a silicotic rat model and MH-S cells induced by SiO<sub>2</sub> to investigate the potential involvement of MMT in

silicosis. The aim was to provide valuable insights for clinical research and therapeutic strategies aimed at assisting silicosis patients.

## 2 | MATERIALS AND METHODS

## 2.1 | Materials

The materials used in the analysis were as hematoxylin and eosin (HE) dye (BA4025, Baso Diagnostics Inc., Zhuhai, China), Van Gieson (VG) dye (BA4084, Baso Diagnostics Inc.), vimentin (ab92547, Abcam, Cambridge, UK),  $\alpha$ -SMA (ET1607-43, HUABIO, Hangzhou, China),  $\alpha$ -SMA (ab5694, Abcam), type I collagen (Col I) (ab34710, Abcam), Col I (ARG21965, Arigo Biolaboratories, Taiwan, China), F4/80 (RT1212, HA721520, HUABIO), CD206 (sc58986, Santa Cruz Biotechnology, Dallas, TX, USA), iNOS (ARG56509, Arigo Biolaboratories), Arg (ab91279, Abcam),  $\beta$ -actin (AC026, ABclonal Biotechnology), ECL prime Western blotting detection reagent (ZD310A, ZomanBio, Beijing, China), SiO<sub>2</sub> (s5631, Sigma, MD, USA), HOPE MED 8050 exposure control apparatus (HOPE Industry and Trade Co. Ltd., Tianjin, China), and SPSS, version 20.0, software (IBM Corp., NY, USA).

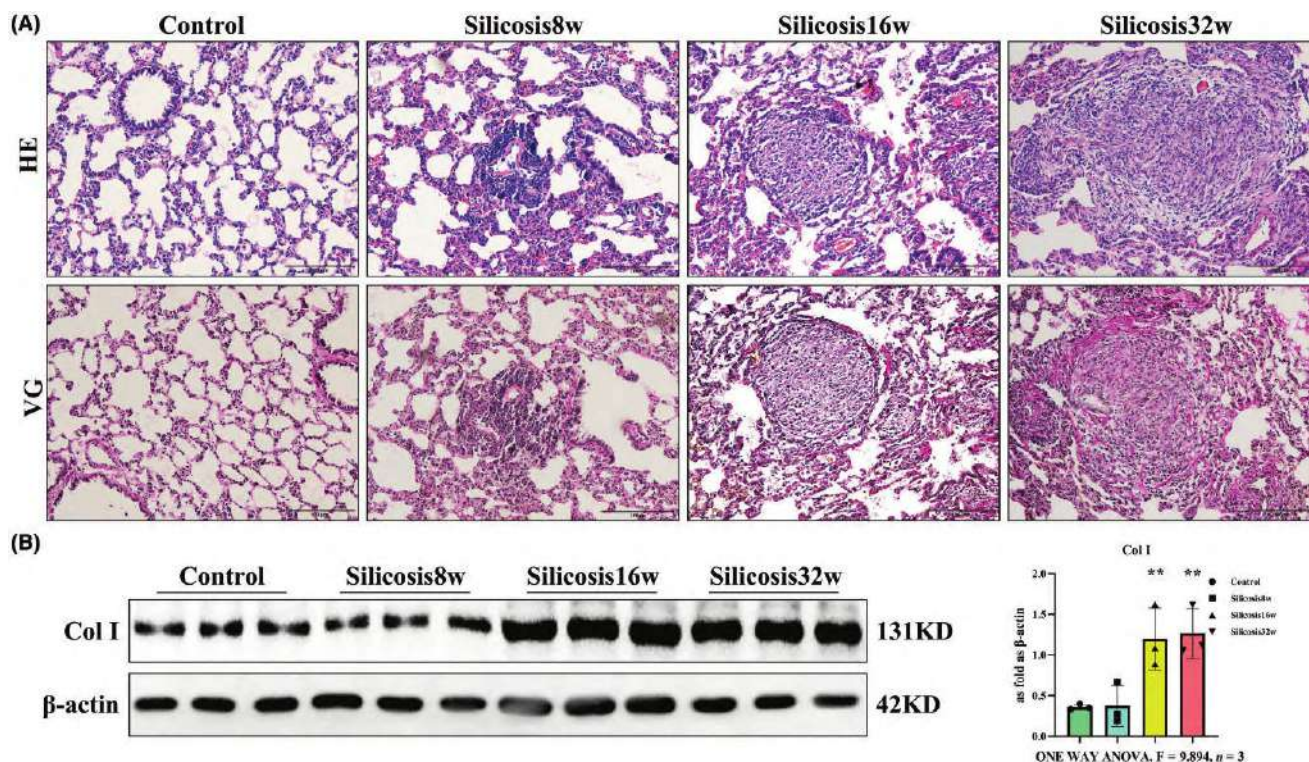


FIGURE 1 Evaluation of the silicosis rat model. (A) HE (hematoxylin and eosin) staining and VG (Van Gieson) staining (bar = 100  $\mu$ m). (B) Western blot measurement of Col I (type I collagen). \*\* $p$  < 0.01.

## 2.2 | Animal experiments

To develop the silicotic rat model, the HOPE MED 8050 exposure control apparatus was utilized. The chamber conditions were maintained as follows: temperature within the range of 20–25°C, humidity levels at 70%–75%, pressure ranging from –50 to +50 Pa, an oxygen concentration of 20%, and an SiO<sub>2</sub> delivery rate of 3.0–3.5 mL/min.<sup>12</sup>

Rats were randomly divided into the following groups ( $n=10$ ): control group and silicosis group (rats were exposed to

silica [ $50 \pm 10 \text{ mg/m}^3$ ] for 3 h/day). The rats were killed at 8, 16, and 32 weeks, and lung tissue and bronchoalveolar lavage fluid (BALF) were collected using a standard technique for the following tests.

## 2.3 | Cell experiments

Murine macrophage MH-S cells were grown in F12K medium containing 10% fetal bovine serum. MH-S cells were randomly divided into a control group and an SiO<sub>2</sub> group.

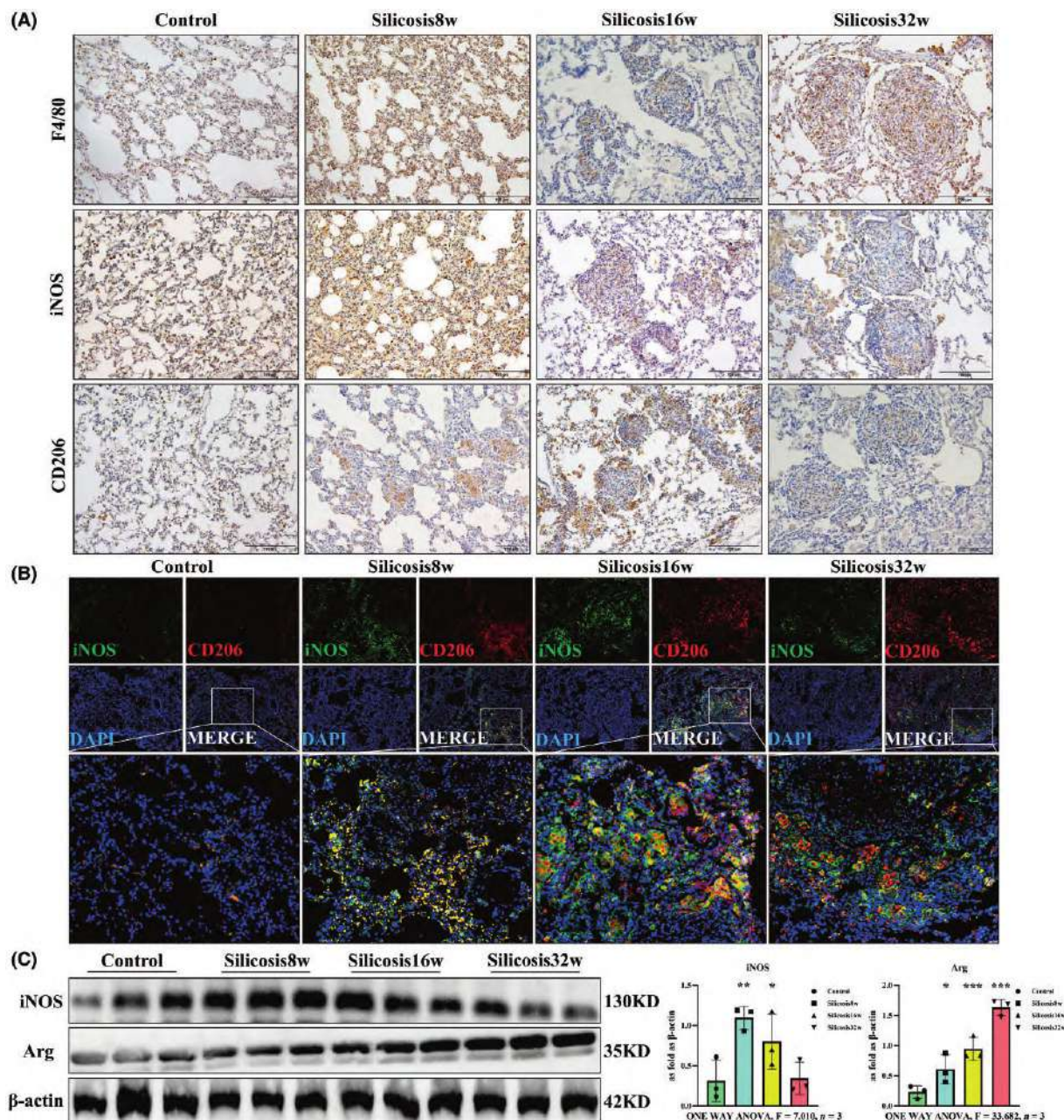


FIGURE 2 Macrophage polarization in silicosis rat model. (A) Immunohistochemistry of F4/80, iNOS, and CD206 (bar = 100  $\mu\text{m}$ ). (B) Immunofluorescence of iNOS and CD206 (bar = 200  $\mu\text{m}$ ). (C) Western blot measurement of iNOS and Arg levels in the lungs. \* $p < 0.05$ , \*\* $p < 0.01$ , and \*\*\* $p < 0.001$ .

## 2.4 | Histology staining

The paraffin-embedded tissue was cut into ~5- $\mu$ m-thick sections. After deparaffinization and rehydration, the sections were treated with hematoxylin and then with eosin dye to observe the pathological morphology.

The slices were treated with the same amount of a mixed solution of hematoxylin A and hematoxylin B for 3 min. Subsequently, VG dye was applied to the sections to observe collagen deposition.

## 2.5 | Immunostaining

The dewaxed tissue sections were treated with 3% hydrogen peroxide solution, and then antigen retrieval was performed using the high-pressure method. The tissues were incubated with primary antibodies against  $\alpha$ -SMA, vimentin, and Col I overnight after blocking with 5% bovine serum albumin. Subsequently, the sections were exposed to the respective secondary antibody before the application of Diaminobenzidine. The slices were observed using light microscopy, where positive results were indicated by brown staining.

$\alpha$ -SMA/F4/80,  $\alpha$ -SMA/CD206, and  $\alpha$ -SMA/F4/80/Col I were co-stained. The sections were incubated overnight with secondary antibody. To stain the nuclei, Diaminidine phenyl indole (DAPI) was utilized.

## 2.6 | Western blot

Western blotting was carried out according to the original protocol.<sup>13</sup>

The proteins extracted from lung tissues and MH-S cells were separated using sodium dodecyl sulfate-polyacrylamide gels and then transferred onto polyvinylidene fluoride (PVDF) membranes. These membranes were subsequently treated with primary antibodies, including F4/80, iNOS, Arg,  $\alpha$ -SMA, vimentin, Col I, and  $\beta$ -actin. Then, the membranes were incubated with secondary antibodies. Subsequently, ECL prime Western blotting detection reagent was used to observe the PVDF membrane, and the results were normalized with the corresponding control.

## 2.7 | Statistical analysis

SPSS, version 20.0, software was used for statistical analysis. Data were expressed as the mean  $\pm$  standard deviation. Two-group comparisons were performed using the independent *t*-test, whereas multiple group comparisons were performed using one-way analysis of variance. *p* < 0.05 was considered statistically significant.

## 3 | RESULTS

### 3.1 | Evaluation of the silicosis rat model

To assess the validity of the silicosis rat model, the histopathological changes in the lungs were observed using HE and VG staining. The lung tissue in control rats consisted of slender alveolar structures and intact capillary walls. Compared with control rats, rats in the 8-week silicosis group exhibited significant inflammatory reaction, with thickening of the alveolar walls and formation of some small

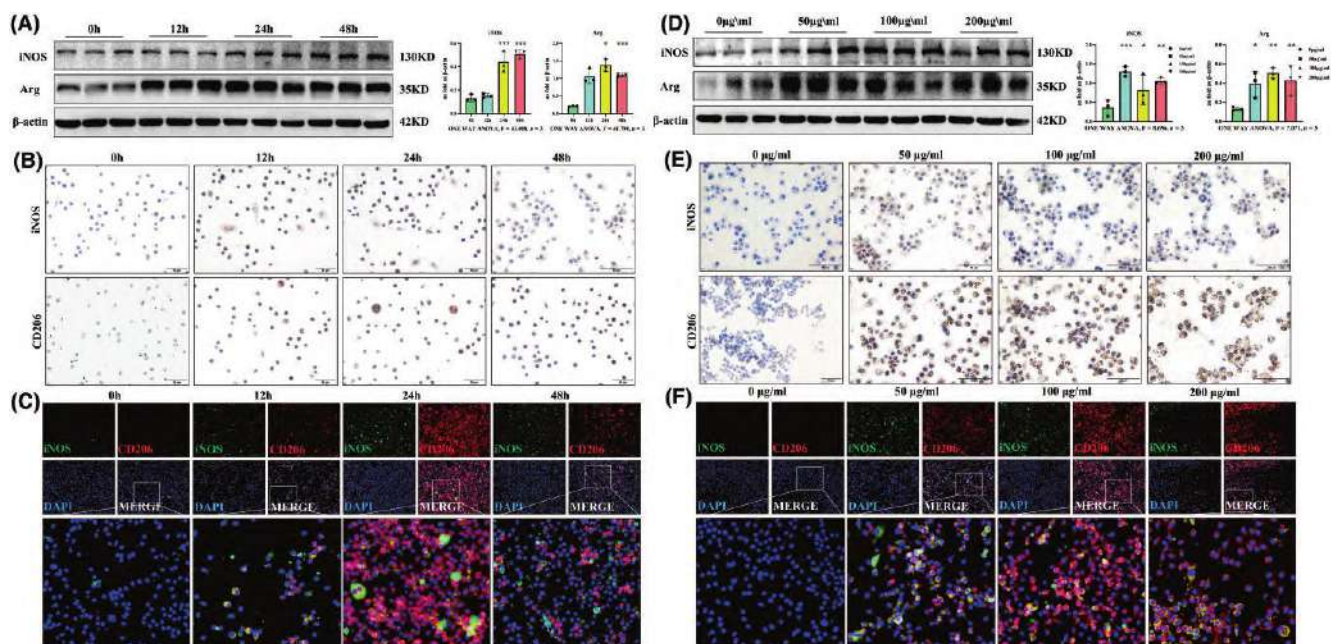


**FIGURE 3** Macrophage polarization in MH-S cell induced by SiO<sub>2</sub>. (A,D) Western blot measurement of iNOS and Arg levels in MH-S cell. (B,E) Immunocytochemical staining of iNOS and CD206 (bar = 50  $\mu$ m). (C,F) Immunofluorescence of iNOS and CD206 (bar = 100  $\mu$ m). \**p* < 0.05, \*\**p* < 0.01, and \*\*\**p* < 0.001.

cellular nodules. Scattered larger nodules were observed in the lungs of 16-week silicosis rats. The lungs exhibited extensive fibrosis with silicotic nodules and increased collagen fiber deposition at

32 weeks (Figure 1A). Similar results were also found for Col I in different groups using Western blotting (Figure 1B). The aforementioned results established the silicosis rat model.

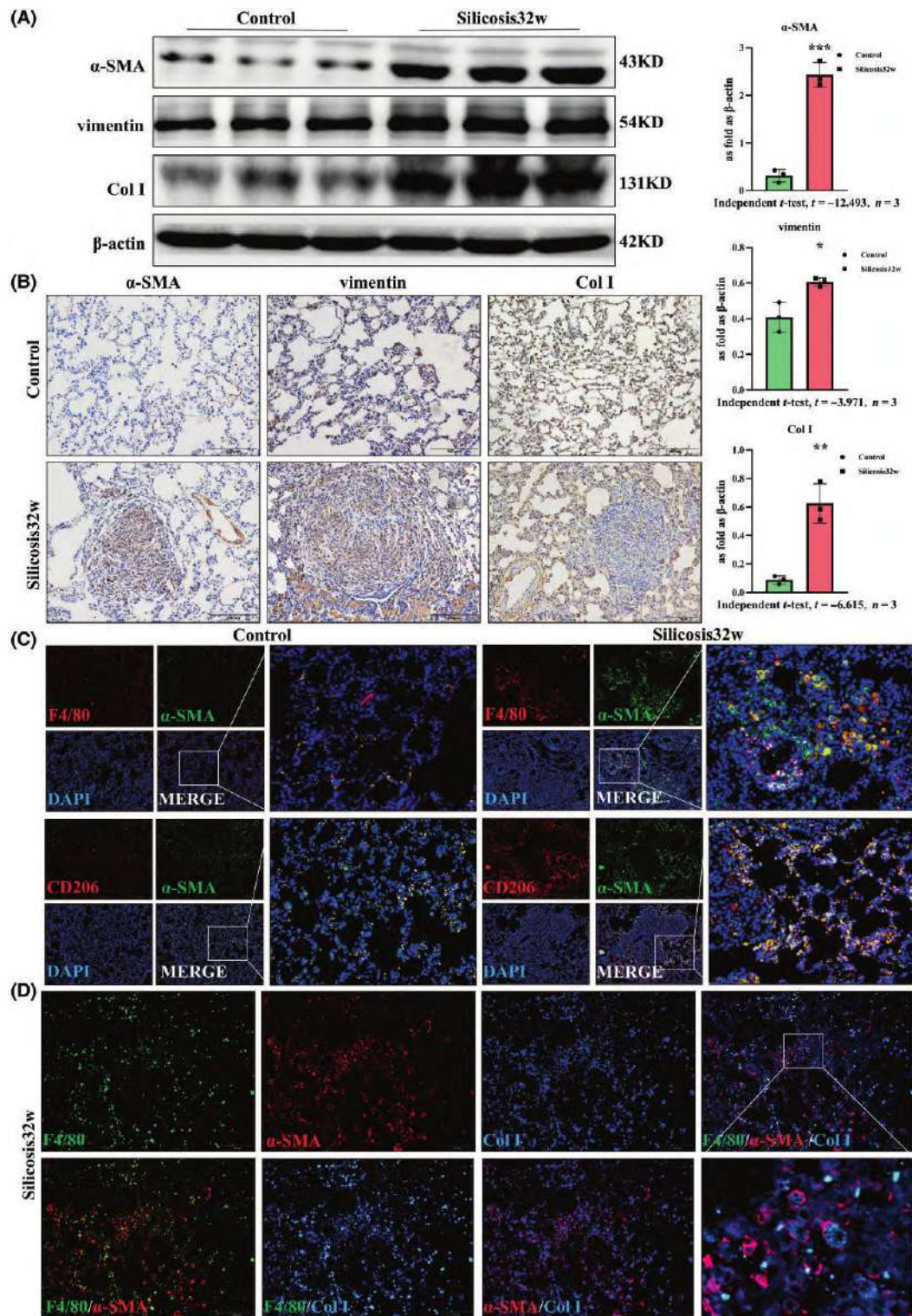


**FIGURE 4** MMT (macrophage-to-myofibroblast transition) in silicosis rat model. (A) Western blot measurement of  $\alpha$ -SMA ( $\alpha$ -smooth muscle Actin), vimentin, and Col I (type I collagen). (B) Immunohistochemistry of  $\alpha$ -SMA, vimentin, and Col I (bar = 100  $\mu$ m). (C) Immunofluorescence of F4/80, CD206, and  $\alpha$ -SMA (bar = 200  $\mu$ m). (D) Immunofluorescence of F4/80,  $\alpha$ -SMA, and Col I (bar = 100  $\mu$ m). \* $p < 0.05$ , \*\* $p < 0.01$ , and \*\*\* $p < 0.001$ .

### 3.2 | Macrophage polarization in silicosis rats

Macrophages cause the secretion of inflammatory factors and pro-fibrotic factors, accelerating the development of fibrosis.<sup>4,5</sup> F4/80, a marker for macrophage, was found in the fibrotic area using immunohistochemistry and increased gradually from 8 to 32 weeks (Figure 2A).

Particularly, macrophage polarization can affect the process of lung fibrosis, especially tissue repair, regeneration, and fibrosis. To study the effects of macrophage polarization on silicosis, the expressions of macrophage signature factors, including the M1 macrophage factor iNOS and the M2 macrophage factor CD206, were detected at various times throughout the development of silicosis using immunohistochemistry and immunofluorescence techniques. The results consistently indicated a higher expression level of iNOS in M1 macrophages compared with CD206 in M2 macrophages at 8 weeks. The gradual increase in the level of M2 macrophage factor (CD206) as fibrosis progressed suggests the significance of M2 macrophages in the fibrotic stage (Figure 2A,B). Consistent with the pathological results, Western blot showed that the levels of

M1 (iNOS) and M2 (Arg) increased in the silicosis group compared with the control group. The maximum level of iNOS was reached at 8 weeks and declined slightly but remained higher than the normal level. The level of Arg gradually increased and peaked at 32 weeks. These results show that M1 macrophages predominated in the early phase of inflammation, whereas M2 macrophages predominated in the late phase of fibrosis (Figure 2C).

### 3.3 | Macrophage polarization in MH-S induced by SiO<sub>2</sub>

Consistent with the findings of silicosis rats, the results of MH-S induced by SiO<sub>2</sub> demonstrated that SiO<sub>2</sub> could induce macrophage polarization. Figure 3 shows that the levels of iNOS, CD206, or Arg were upregulated in MH-S treated with SiO<sub>2</sub> for 24 and 48 h (Figure 3A–C). The levels of iNOS and CD206 and Arg treated with 50, 100, and 200 μg/mL of SiO<sub>2</sub> for 24 h were elevated (Figure 3D–F).

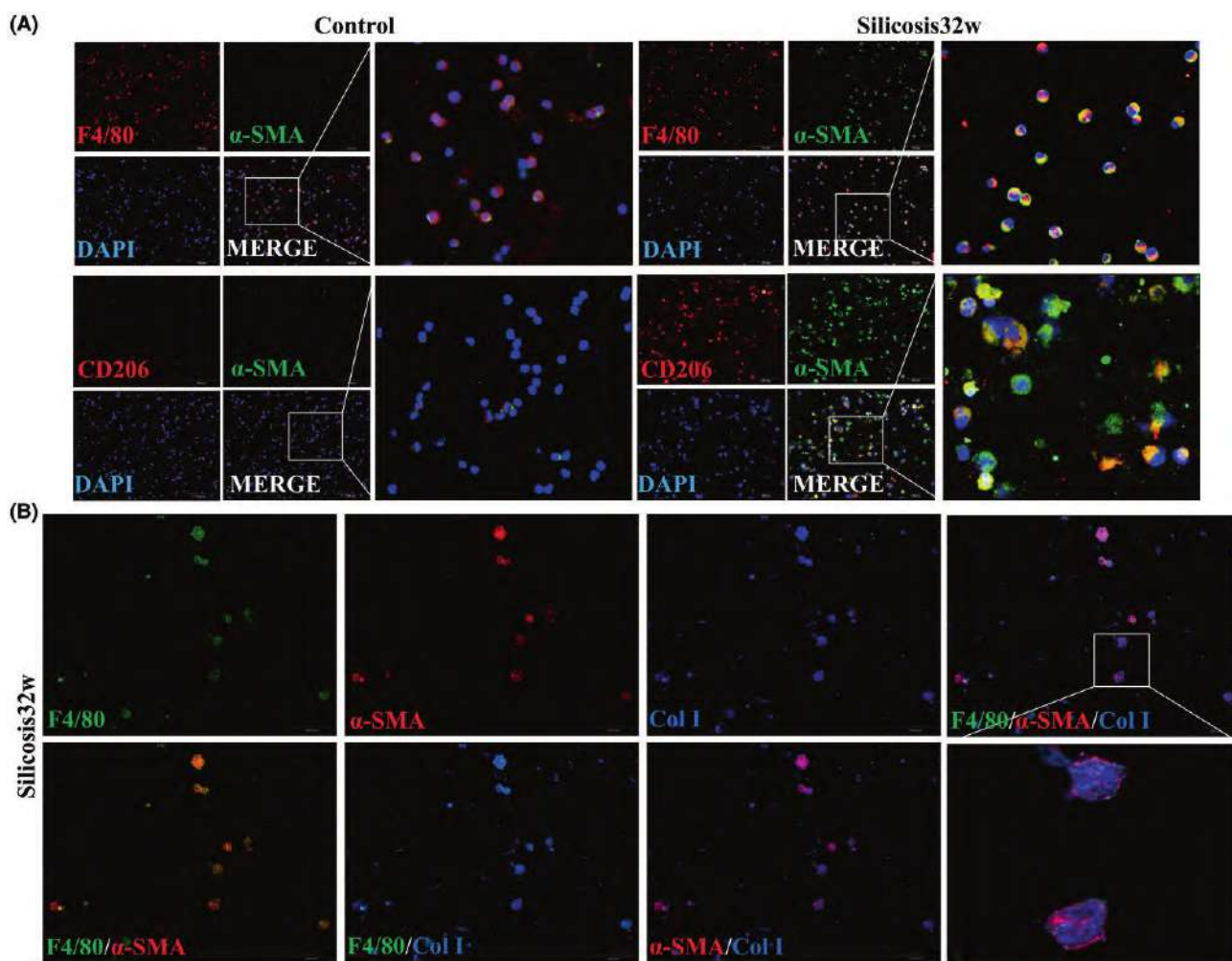


**FIGURE 5** MMT (macrophage-to-myofibroblast transition) in the BALF (bronchoalveolar lavage fluid) from silicosis rat. (A) Immunofluorescence of F4/80, CD206, and  $\alpha$ -SMA ( $\alpha$ -smooth muscle Actin) (bar = 100  $\mu$ m). (B) Immunofluorescence of F4/80,  $\alpha$ -SMA, and Col I (bar = 100  $\mu$ m).

### 3.4 | MMT in silicosis rats

Recent studies have demonstrated that the MMT, characterized by co-expression of myofibroblast and macrophage markers, contributes to

fibrosis.<sup>6-11</sup> Immunohistochemistry and Western blotting revealed that the levels of  $\alpha$ -SMA and vimentin, specific myofibroblast markers, increased in silicosis rats compared with those in control rats (Figure 4A,B). Next, an attempt was made to perform immunofluorescence co-staining

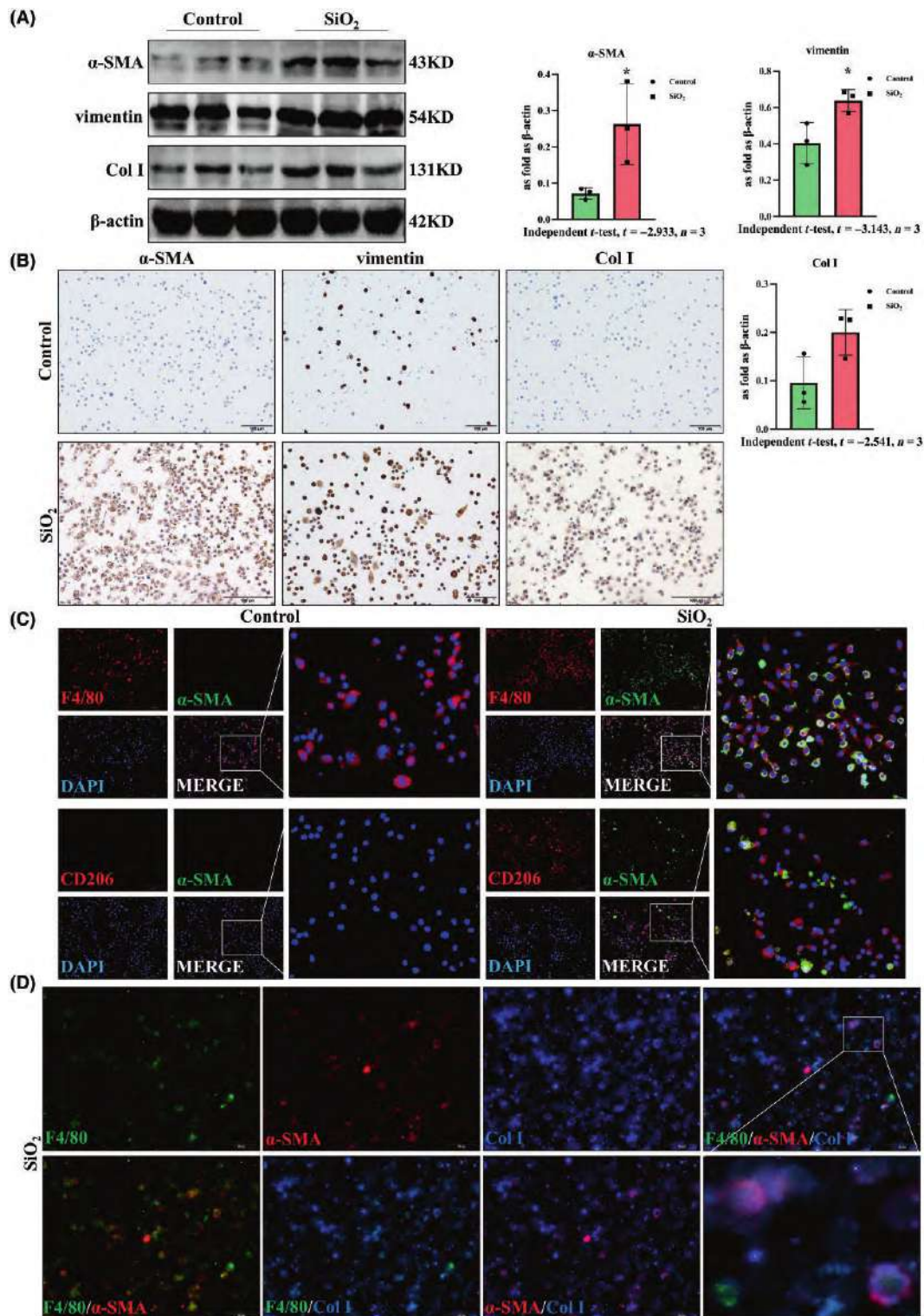


**FIGURE 6** MMT (macrophage-to-myofibroblast transition) in MH-S cells induced by  $\text{SiO}_2$ . (A) Western blot measurement of  $\alpha$ -SMA ( $\alpha$ -smooth muscle Actin), vimentin, and Col I (type I collagen). (B) Immunocytochemical staining of  $\alpha$ -SMA, vimentin, and Col I (bar = 100  $\mu\text{m}$ ). (C) Immunofluorescence of F4/80, CD206, and  $\alpha$ -SMA (bar = 100  $\mu\text{m}$ ). (D) Immunofluorescence of F4/80,  $\alpha$ -SMA, and Col I (bar = 50  $\mu\text{m}$ ). \* $p < 0.05$ .

of the myofibroblast marker  $\alpha$ -SMA and the macrophage marker F4/80. As expected, the number of F4/80<sup>+</sup> $\alpha$ -SMA<sup>+</sup> cells in the silicosis group was higher, indicating the occurrence of MMT (Figure 4C). The level of Col I, the main component of the extracellular matrix, was higher in the silicosis group (Figure 4A). Meanwhile, the cells expressing both F4/80 and  $\alpha$ -SMA also co-expressed Col I, suggesting that MMT cells regulate fibrosis mainly by producing collagen (Figure 4D). Moreover, subtypes of macrophages contributing to MMT were explored by co-expressing  $\alpha$ -SMA and the M2 macrophage marker CD206 (Figure 4C). The results further revealed that M2 macrophages are the major contributors to MMT in silicosis rats.

The same results were found in the BALF from control and silicosis rats. Consistent with our previous findings, F4/80<sup>+</sup> $\alpha$ -SMA<sup>+</sup> or CD206<sup>+</sup> $\alpha$ -SMA<sup>+</sup> cells in the 32-week silicosis group increased (Figure 5A). Meanwhile, the cells expressing both F4/80 and  $\alpha$ -SMA also co-expressed Col I (Figure 5B).

### 3.5 | MMT in MH-S induced by SiO<sub>2</sub>

MH-S was cultured with SiO<sub>2</sub> (50  $\mu$ g/mL) for 24 h to observe changes in MMT. Consistent with the pathological observations, the levels of  $\alpha$ -SMA, vimentin, and Col I were upregulated in the SiO<sub>2</sub> group (Figure 6A,B). The macrophages co-expressing with F4/80 or CD206 and  $\alpha$ -SMA underwent a myofibroblast-like spindle morphological transformation (Figure 6C). Furthermore, analysis of three-color immunofluorescence revealed that F4/80<sup>+</sup> $\alpha$ -SMA<sup>+</sup> cells also expressed Col I (Figure 6D). This suggests that SiO<sub>2</sub>-induced MMT led to a phenotypic transformation, where these cells secreted collagen components, contributing to the development of silicosis.

## 4 | DISCUSSION

Pulmonary macrophages are the innate immune cells that play a role in the pathogenesis of fibrosis due to their characteristics such as phagocytosis, immunological function, and secretion function.<sup>14,15</sup> In general, macrophages can be broadly divided into two populations, namely classically activated macrophages (M1 macrophages) and alternatively activated macrophages (M2 macrophages). M1 macrophages promote inflammation, whereas M2 macrophages enhance tissue repair and fibrosis.<sup>16–18</sup> To explore the role of macrophage polarization in silicosis, the silicotic rat model was developed using the HOPE MED 8050 exposure control apparatus. Pathological changes observed using the HE and VG staining methods at various times revealed that the lungs of silicosis rats exhibited the infiltration of substantial inflammatory cells, the thickening of alveolar walls, and the formation of silicon nodules. The results showed that the level of M1 marker significantly increased in the early stages of silicosis. Furthermore, the expression level of the M2 marker reached the peak at 32 weeks of silica exposure, which includes the early inflammatory phase

characterized by M1 macrophages and the late fibrotic phase characterized by M2 macrophages.

It is widely known that myofibroblasts, expression of  $\alpha$ -SMA, are the principal mediators of tissue fibrosis, accounting for the elevated collagen production.<sup>19</sup> Myofibroblasts represent a diverse population from different cell sources, including local proliferation of resident fibroblasts or pericytes, epithelial–mesenchymal transition, and endothelial–mesenchymal transition.<sup>20–23</sup> Recent studies have underscored the significance of MMT as a pivotal pathway for myofibroblast accumulation. MMT may play a key regulatory role in fibrotic diseases, including renal fibrosis,<sup>24–28</sup> subretinal fibrosis,<sup>29,30</sup> cardiac fibrosis,<sup>31–33</sup> skeletal muscle fibrosis,<sup>34</sup> liver fibrosis,<sup>35</sup> peritoneal fibrosis,<sup>36</sup> and pulmonary fibrosis.<sup>13,28,37</sup> In the present study, the correlation among macrophages and the progress of silicosis rats was validated. Notably, F4/80<sup>+</sup> $\alpha$ -SMA<sup>+</sup> MMT cells constituted a significant portion of silicosis, contributing substantially to collagen I production. Additionally, it was observed that the most of these MMT cells expressed the M2 marker CD206, which is consistent with similar findings related to MMT cells in the kidney. These outcomes corroborated with the MH-S cells induced by SiO<sub>2</sub>, thereby confirming the involvement of MMT by M2 macrophages in lung fibrosis.

## 5 | CONCLUSIONS

In conclusion, this study has identified that MMT may be an important pathway, and it may contribute to the development of silicosis. This transition predominantly involves M2 macrophages and deposition of collagen I. Activation of MMT may be a crucial regulatory mechanism of silicosis.

### AUTHOR CONTRIBUTIONS

Fei Geng, Jingrou Xu, Xichen Ren, Na Mao, Ying Sun, and Fang Yang: conceptualization; Fei Geng, Jingrou Xu, and Xichen Ren: methodology; Fei Geng, Ying Zhao, and Yuhao Cai: software; Yaqian Li, Tian Li, and Fuyu Jin: validation; Xuemin Gao and Wenchen Cai: data curation; Fei Geng and Zhongqiu Wei: writing—original draft preparation; Hong Xu, Na Mao, and Fang Yang: writing—review; Na Mao, Ying Sun, and Fang Yang: supervision; Xuemin Gao, Zhongqiu Wei, and Ying Sun: funding acquisition.

### ACKNOWLEDGMENTS

We would like to thank Editor (<https://www.editorbar.com>) for editing the English text of a draft of this manuscript.

### FUNDING INFORMATION

The National Natural Science Foundation of China (no. 82204006), the Science and Technology of Project of Hebei Education Department (QN2022009), the Provincial Graduate Student Innovation Funding Project of Hebei Province (CXZZBS2022104), and the National Natural Science Foundation of Hebei Province (H2020209292).

## CONFLICT OF INTEREST STATEMENT

The authors declare no conflict of interest.

## ETHICS STATEMENT

The animal experiments were conducted in accordance with the guidelines set by the Animal Management and Use Committee of North China University of Science and Technology (Tangshan, China; Protocol No. LX 2019033, LX2019035, SQ2022025).

## ORCID

Hong Xu  <https://orcid.org/0000-0002-3655-3833>

Zhongqiu Wei  <https://orcid.org/0000-0002-1895-7295>

## REFERENCES

- Handra CM, Gurzu IL, Chirila M, Ghita I. Silicosis: new challenges from an old inflammatory and fibrotic disease. *Front Biosci*. 2023;28(5):96.
- Ryan FH, Daniel CC. Silica-related diseases in the modern world. *Allergy*. 2020;75(11):2805-2817.
- Li T, Yang XY, Xu H, Liu H. Early identification, accurate diagnosis, and treatment of silicosis. *Can Respir J*. 2022;2022:3769134.
- Amit K, Martin P. Roles of macrophage polarization and macrophage-derived miRNAs in pulmonary fibrosis. *Front Immunol*. 2021;12:678457.
- Yang HD, Cheng H, Dai RR, Shang L, Zhang X, Wen H. Macrophage polarization in tissue fibrosis. *PeerJ*. 2023;11:e16092.
- Wei J, Xu ZH, Yan X. The role of the macrophage-to-myofibroblast transition in renal fibrosis. *Front Immunol*. 2022;13:934377.
- Vierhout M, Ayoub A, Naiel S, et al. Monocyte and macrophage derived myofibroblasts: is it fate? A review of the current evidence. *Wound Repair Regen*. 2021;29(4):548-562.
- Meng XM, Thomas SKM, Lan HY. Macrophages in renal fibrosis. *Adv Exp Med Biol*. 2019;1165:285-303.
- Paterson DJN, Wang S, Lan HY. Macrophages promote renal fibrosis through direct and indirect mechanisms. *Kidney Int Suppl*. 2014;4(1):34-38.
- Wang S, Meng XM, Ng YY, et al. TGF- $\beta$ /Smad3 signalling regulates the transition of bone marrow-derived macrophages into myofibroblasts during tissue fibrosis. *Oncotarget*. 2016;7(8):8809-8822.
- Meng XM, Wang S, Huang XR, et al. Inflammatory macrophages can transdifferentiate into myofibroblasts during renal fibrosis. *Cell Death Dis*. 2016;7(12):e2495.
- Li YQ, Jin FY, Li T, et al. Minute cellular nodules as early lesions in rats with silica exposure via inhalation. *Vet Sci*. 2022;9(6):1-10.
- Geng F, Zhao L, Cai YH, et al. Quercetin alleviates pulmonary fibrosis in Silicotic mice by inhibiting macrophage transition and TGF- $\beta$ -Smad2/3 pathway. *Curr Issues Mol Biol*. 2023;45(4):3087-3101.
- Cheng PY, Li SY, Chen HY. Macrophages in lung injury, repair, and fibrosis. *Cells*. 2021;10(2):1-10.
- Lee JW, Chun WJ, Lee HJ, et al. The role of macrophages in the development of acute and chronic inflammatory lung diseases. *Cells*. 2021;10(4):1-9.
- Shweta A, Kapil D, Beamon A, et al. Macrophages: their role, activation and polarization in pulmonary diseases. *Immunobiology*. 2018;223(4-5):383-396.
- Elza E, Emma R, Tim W. Origin and ontogeny of lung macrophages: from mice to humans. *Immunology*. 2020;160(2):126-138.
- Deng LS, Jian ZJ, Xu T, et al. Macrophage polarization: an important candidate regulator for lung diseases. *Molecules (Basel, Switzerland)*. 2023;28(5):1-10.
- Liu G, Ashleigh MP, Tamera C, et al. Therapeutic targets in lung tissue remodelling and fibrosis. *Pharmacol Ther*. 2021;225:107839.
- Shoichiro S, Masahiro K, Noriko OS, et al. Angiotensin-like 4 is a critical regulator of fibroblasts during pulmonary fibrosis development. *Am J Respir Cell Mol Biol*. 2023;69(3):328-339.
- Ren ZN, Pan XH, Li JH, et al. G protein coupled receptor 41 regulates fibroblast activation in pulmonary fibrosis via  $G\alpha_i$  and downstream Smad2/3 and ERK1/2 phosphorylation. *Pharmacol Res*. 2023;191:106754.
- Li SM, Li YQ, Xu H, et al. ACE2 attenuates epithelial-mesenchymal transition in MLE-12 cells induced by silica. *Drug Des Devel Ther*. 2020;14:1547-1559.
- Liu SP, Jin RT, Zheng GG, et al. Ac-SDKP promotes KIF3A-mediated  $\beta$ -catenin suppression through a ciliary mechanism to constrain silica-induced epithelial-myofibroblast transition. *Biomed Pharmacother*. 2023;166:115411.
- Guo QT, Li P, Chen ML, et al. Exosomes from human umbilical cord stem cells suppress macrophage-to-myofibroblast transition, alleviating renal fibrosis. *Inflammation*. 2024;2024:1-10.
- Yu WQ, Song JF, Chen SQ, et al. Myofibroblast-derived exosomes enhance macrophages to myofibroblasts transition and kidney fibrosis. *Ren Fail*. 2024;46(1):2334406.
- Luo LH, Wang SJ, Hu YL, et al. Precisely regulating M2 subtype macrophages for renal fibrosis resolution. *ACS Nano*. 2023;17(22):22508-22526.
- Gao Y, Liu BQ, Guo XQ, et al. Interferon regulatory factor 4 deletion protects against kidney inflammation and fibrosis in deoxycorticosterone acetate/salt hypertension. *J Hypertens*. 2023;41(5):794-810.
- Yang F, Chang Y, Zhang CJ, et al. UUO induces lung fibrosis with macrophage-myofibroblast transition in rats. *Int Immunopharmacol*. 2021;93:107396.
- Yi CJ, Liu J, Deng W, et al. Macrophage elastase (MMP12) critically contributes to the development of subretinal fibrosis. *J Neuroinflammation*. 2022;19(1):78.
- Karis L, Maria LS, Tang M, et al. Macrophage to myofibroblast transition contributes to subretinal fibrosis secondary to neovascular age-related macular degeneration. *J Neuroinflammation*. 2020;17(1):355.
- Zhuang T, Chen H, Wu RX, et al. ALKBH5-mediated m6A modification of IL-11 drives macrophage-to-myofibroblast transition and pathological cardiac fibrosis in mice. *Nat Commun*. 2024;15(1):1995.
- Shen SC, Zhang M, Wang XH, et al. Single-cell RNA sequencing reveals S100a9hi macrophages promote the transition from acute inflammation to fibrotic remodeling after myocardial ischemia-reperfusion. *Theranostics*. 2024;14(3):1241-1259.
- Han YT, Xian YQ, Gao XM, et al. Eplerenone inhibits the macrophage-to-myofibroblast transition in rats with UUO-induced type 4 cardiorenal syndrome through the MR/CTGF pathway. *Int Immunopharmacol*. 2022;113:109396.
- Qi BJ, Li YQ, Peng Z, et al. Macrophage-myofibroblast transition as a potential origin for skeletal muscle fibrosis after injury via complement system activation. *J Inflamm Res*. 2024;17:1083-1094.
- Xia SH, Huang YJ, Zhang Y, et al. Role of macrophage-to-myofibroblast transition in chronic liver injury and liver fibrosis. *Eur J Med Res*. 2023;28(1):502.
- Shan Y, Yu MS, Dai HB, et al. The role of macrophage-derived exosomes in reversing peritoneal fibrosis: insights from Astragaloside IV. *Phytomedicine*. 2024;129:155683.
- Liu HJ, Guan QZ, Zhao P, Li J. TGF- $\beta$ -induced CCR8 promoted macrophage transdifferentiation into myofibroblast-like cells. *Exp Lung Res*. 2022;4:1-14.

**How to cite this article:** Geng F, Xu J, Ren X, et al. Effect of macrophage-to-myofibroblast transition on silicosis. *Anim Models Exp Med*. 2025;8:363-371. doi:10.1002/ame2.12470